BNL-227920-2025-TECH

CA/AP/718

Modeling wiggler with hard edge dipoles

I. Pinayev

March 2025

Collider Accelerator Department

Brookhaven National Laboratory

U.S. Department of Energy

USDOE Office of Science (SC), Nuclear Physics (NP)

DISCLAIMER

Modeling Wiggler with Hard Edge Dipoles

I. Pinayev
Collider-Accelerator Department, BNL

INTRODUCTION

Wigglers and undulators are used as devices for generating synchrotron radiation. They are also used for mod-ification of various beam properties circulating in a storage ring. Basic 'dumping wiggler' is used for change of the damping time, equilibrium emittance, and energy spread [1-3]. In [1] damping wigglers are used to increase the damping rate of the energy spread induced by the beam-beam interaction. The commonly used MAD [4] and Elegant [5] software has only simplified planar wiggler configuration and no model for a helical wiggler.

WIGGLER MODELS

The model will provide the same transverse focusing and synchrotron radiation power using rectangular bending magnets (no focusing in the deflection plane). The central part of wiggler usually has sinusoidal field distribution on axis (selecting the pole width to sup-press the third harmonic while higher harmonics decay exponentially). For example, in a planar wiggler with peak field $B_{wiggler}$ and period λ_W the transverse components of the magnetic field can be described by formula

$$B_y(s) = B_{wiggler} \sin k_W s$$

where $k_W = \frac{2\pi}{\lambda_w}$.

On axis magnetic field of the helical wiggler (with equal field amplitudes $B_{wiggler}$) is described by

$$B_y(s) = B_{wiggler} \sin k_W s$$
$$B_x(s) = B_{wiggler} \cos k_W s$$

For a planar wiggler each pole can be represented as rectangular dipole with field *Beff* and length D_{eff} separated by drift from other poles. We need to have the same deflection angle and synchrotron radiation power. Hence

$$B_{eff} D_{eff} = \int_0^{\lambda_w/2} B_{wiggler} \sin k_w s \, ds = \frac{B_{wiggler} \lambda_W}{\pi}$$
$$2B_{eff}^2 D_{eff} = \int_0^{\lambda_W} B_{wiggler}^2 \sin^2 k_W s \, ds = \frac{B_{wiggler}^2 \lambda_W}{2}$$

Solving these two equations gives

$$B_{eff} = \frac{\pi B_{wiggler}}{4}$$
$$D_{eff} = \frac{4\lambda_W}{\pi^2}$$

While wiggler with integer number of periods does not provide transverse angular kick (the field integral is zero), it provides the displacement in the deflection plane (the second integral is not zero). The second integral can be set to zero by utilizing the first and the last poles at half strength of the central part. The beam displacement from axis (dispersion) will oscillate from zero to maximal value of $2B_{wiggler}/B\rho k_W^2$, where $B\rho$ is beam rigidity.

$$x(s) = -\frac{B_{wiggler}}{B\rho k_W^2}(1 + \sin k_W s)$$

To remove the offset of the oscillation axis the more elaborate entry and exit sequence can be employed [3]. The first (last) pole is quarter strength of internal poles, and the second (second to last) pole has strength of three quarters. The real and model field profiles as well as beam trajectory are shown in Fig. 1.

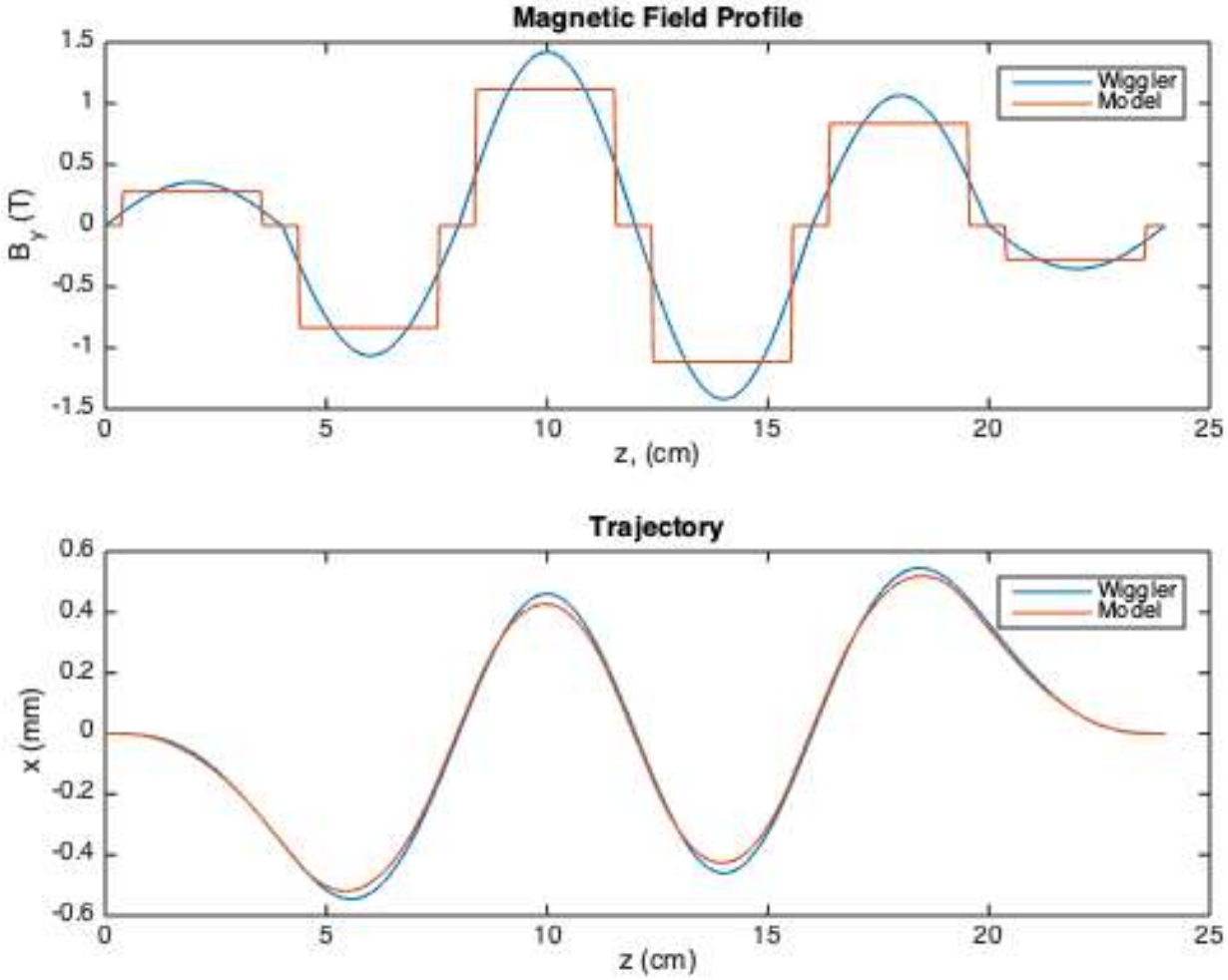

Figure 1: Profiles of the wiggler (blue) and model (red) as well as corresponding trajectories of the beam. The wiggler has only one full strength period in the middle.

A helical wiggler can be modeled with two arrays of the rectangular dipoles shifted by quarter of wiggler period. The first array is comprised of the horizontal dipoles and the second array has vertical dipoles. The field amplitude in the helical wiggler is constant with rotating direction of the field vector. Then the dipole field equal to the wiggler peak field will provide the same power of the synchrotron radiation. The trajectories in the model and wiggler are also close to each other as it can be seen in Figure 2. The difference in the amplitude of transverse motion is 7%.

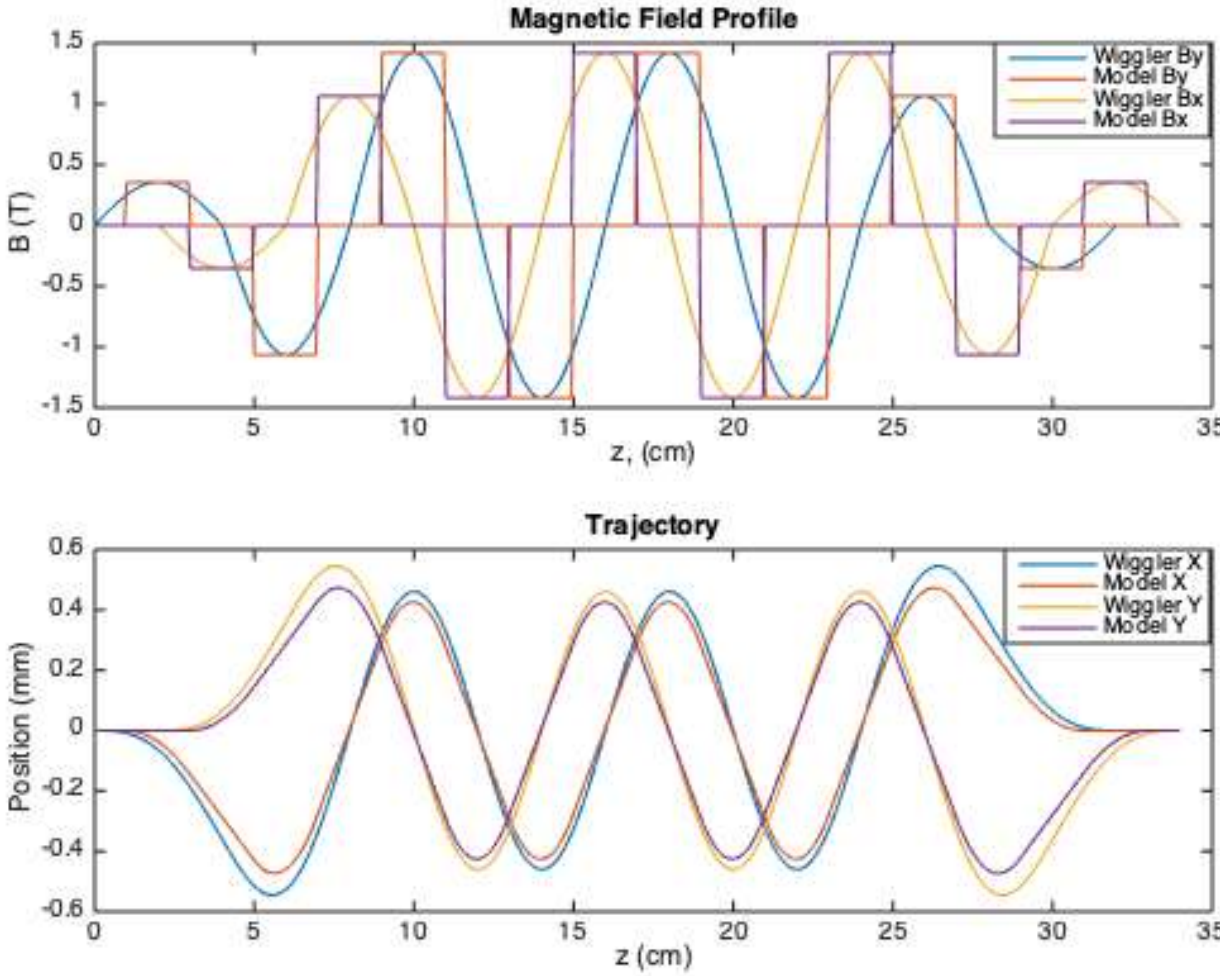

Figure 2: Magnetic fields and beam trajectories in the wiggler and its model.

More precise model of the helical wiggler can be done in similar fashion as for the planar wiggler. The difference will be that now there will be eight dipoles per period (no drifts) with different tilt angles (0, 45, 90, 135, 180, 225, 270, and 315 degrees in the middle) and different amplitudes. Figure 3 shows the field distribution and trajectories while Figure 4 shows the magnetic field amplitude and tilt angle for the model dipoles.

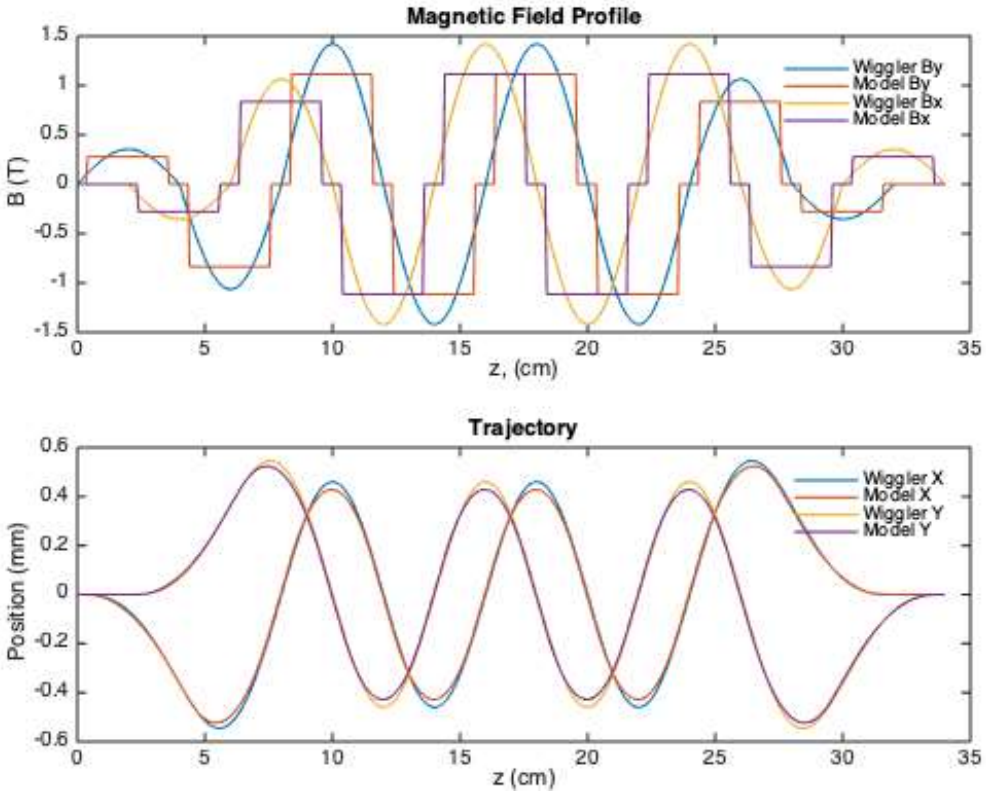

Figure 3: More precise model of the helical wiggler: field and trajectory.

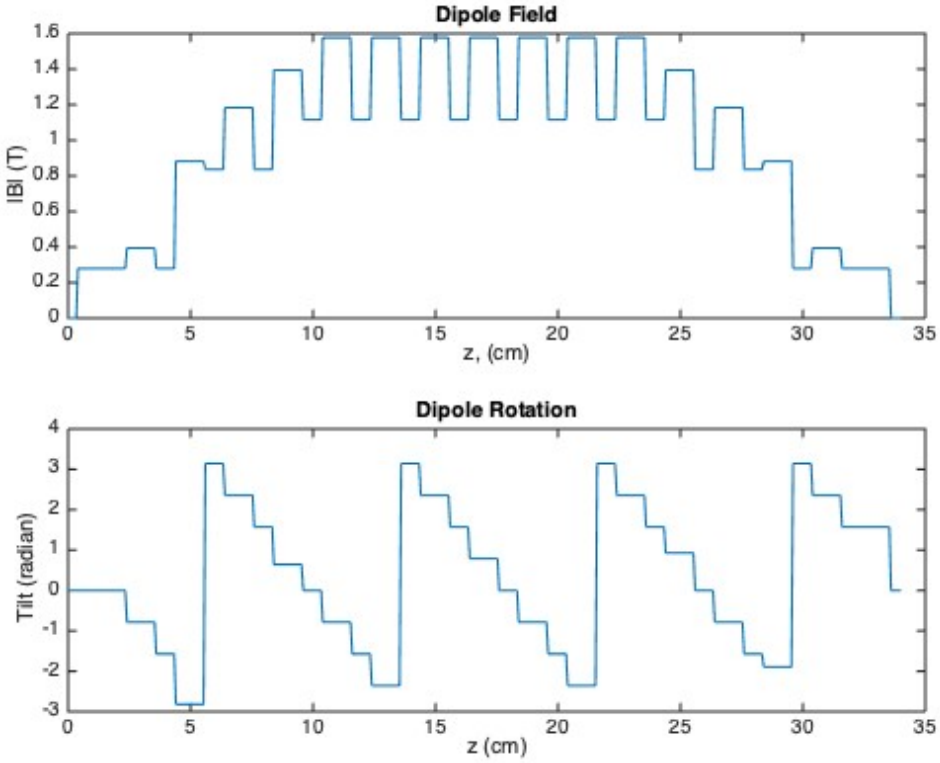

Figure 4: Field amplitudes and tilt angles of the dipoles of more precise model of the helical wiggler.

REFERENCES

[1] H. Zhao, J. Kewisch, M. Blaskiewicz, and A. Fedotov, "Ring-based electron cooler for high energy beam cooling", Physical Review Accelerators and Beams 24, 043501 (2021)
[2] H. Widemann, "An ultra-low emittance mode for PEP using damping wigglers", Nucl. Instr. Meth. NIMA266 (1988), pp. 24-31.
[3] R. Walker, Wigglers, in CERN Accelerator School Proceedings, CERN 95-06, pp. 807-835, http://cds.cern.ch/record/254747/files/CERN-95-06-V1-V2.pdf?version=2
[4] https://ops.aps.anl.gov/manuals/elegant_latest/elegant.html
[5] https://mad.web.cern.ch/mad/webguide/manual.html

APPENDIX Example of Beamline

1. DRIFT, L = $(1-8/\pi^2)/4\ \lambda_W$
2. RBEND, L = ¼ λ_W, B = $\pi/16\ B_W$, TILT = 0.0
3. RBEND, L = $(4/\pi^2-¼)\ \lambda_W$, B = $\pi\sqrt{2}/16\ B_W$, TILT = $-\pi/4$
4. RBEND, L = $(½-4/\pi^2)\ \lambda_W$, B = $\pi/16\ B_W$, TILT = $-\pi/2$
5. RBEND, L = $(4/\pi^2-¼)\ \lambda_W$, B = $\pi\sqrt{10}/16\ B_W$, TILT = ATAN(1/3) - π
6. RBEND, L = $(½-4/\pi^2)\ \lambda_W$, B = $3\pi/16\ B_W$, TILT = π
7. RBEND, L = $(4/\pi^2-¼)\ \lambda_W$, B = $3\pi\sqrt{2}/16\ B_W$, TILT = $3\pi/4$
8. RBEND, L = $(½-4/\pi^2)\ \lambda_W$, B = $3\pi/16\ B_W$, TILT = $\pi/2$
9. RBEND, L = $(4/\pi^2-¼)\ \lambda_W$, B = $5\pi/16\ B_W$, TILT = ATAN(3/4)
10. RBEND, L = $(½-4/\pi^2)\ \lambda_W$, B = $\pi/4\ B_W$, TILT = 0.0
11. RBEND, L = $(4/\pi^2-¼)\ \lambda_W$, B = $\pi\sqrt{2}/4\ B_W$, TILT = $-\pi/4$
12. RBEND, L = $(½-4/\pi^2)\ \lambda_W$, B = $\pi/4\ B_W$, TILT = $-\pi/2$
13. RBEND, L = $(4/\pi^2-¼)\ \lambda_W$, B = $\pi\sqrt{2}/4\ B_W$, TILT = $-3\pi/4$
14. RBEND, L = $(½-4/\pi^2)\ \lambda_W$, B = $\pi/4\ B_W$, TILT = π
15. RBEND, L = $(4/\pi^2-¼)\ \lambda_W$, B = $\pi\sqrt{2}/4\ B_W$, TILT = $3\pi/4$
16. RBEND, L = $(½-4/\pi^2)\ \lambda_W$, B = $\pi/4\ B_W$, TILT = $\pi/2$
17. RBEND, L = $(4/\pi^2-¼)\ \lambda_W$, B = $\pi\sqrt{2}/4\ B_W$, TILT = $\pi/4$
18. RBEND, L = $(½-4/\pi^2)\ \lambda_W$, B = $\pi/4\ B_W$, TILT = 0.0
19. RBEND, L = $(4/\pi^2-¼)\ \lambda_W$, B = $\pi\sqrt{2}/4\ B_W$, TILT = $-\pi/4$
20. RBEND, L = $(½-4/\pi^2)\ \lambda_W$, B = $\pi/4\ B_W$, TILT = $-\pi/2$
21. RBEND, L = $(4/\pi^2-¼)\ \lambda_W$, B = $\pi\sqrt{2}/4\ B_W$, TILT = $-3\pi/4$
22. RBEND, L = $(½-4/\pi^2)\ \lambda_W$, B = $\pi/4\ B_W$, TILT = π
23. RBEND, L = $(4/\pi^2-¼)\ \lambda_W$, B = $\pi\sqrt{2}/4\ B_W$, TILT = $3\pi/4$
24. RBEND, L = $(½-4/\pi^2)\ \lambda_W$, B = $\pi/4\ B_W$, TILT = $\pi/2$
25. RBEND, L = $(4/\pi^2-¼)\ \lambda_W$, B = $5\pi/16\ B_W$, TILT = ATAN(5/4)
26. RBEND, L = $(½-4/\pi^2)\ \lambda_W$, B = $3\pi/16\ B_W$, TILT = 0.0
27. RBEND, L = $(4/\pi^2-¼)\ \lambda_W$, B = $3\pi\sqrt{2}/16\ B_W$, TILT = $-\pi/4$
28. RBEND, L = $(½-4/\pi^2)\ \lambda_W$, B = $3\pi/16\ B_W$, TILT = $-\pi/2$
29. RBEND, L = $(4/\pi^2-¼)\ \lambda_W$, B = $\pi\sqrt{10}/16\ B_W$, TILT = ATAN(3)-π
30. RBEND, L = $(½-4/\pi^2)\ \lambda_W$, B = $\pi/16\ B_W$, TILT = π

31. RBEND, L = $(4/\pi^2-¼)\ \lambda_W$, B = $\pi\sqrt{2}/16\ B_W$, TILT = $3\pi/4$
32. RBEND, L = $¼\ \lambda_W$, B = $\pi/16\ B_W$, TILT = $\pi/2$
33. DRIFT, L = $(1-8/\pi^2)/4\ \lambda_W$

Lines 1-9 correspond to the wiggler entrance, lines 25-33 correspond to the wiggler exit, lines 10-24 form middle of the wiggler (periodicity is 8 lines). The drifts in the first and the last lines can be omitted (they are added to calculate wiggler length equal to the wiggler with sinusoidal field $(N_{periods}+1/4)\lambda_W$).